Materials Reports: Energy 1 (2021) 100021

Contents lists available at ScienceDirect

Materials Reports: Energy

journal homepage: www.keaipublishing.com/en/journals/materials-reports-energy

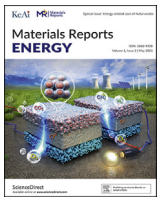

Communication

The first observation of Ni nanoparticle exsolution from YSZ and its application for dry reforming of methane

Sangwook Joo [a,1], Chaehyun Lim [a,1], Ohhun Kwon [a], Linjuan Zhang [b], Jing Zhou [b], Jian-Qiang Wang [b], Hu Young Jeong [c], Yong-wook Sin [d], Sihyuk Choi [e,**], Guntae Kim [a,*]

[a] Department of Energy Engineering, Ulsan National Institute of Science and Technology (UNIST), Ulsan, 698-798, Republic of Korea
[b] Key Laboratory of Interfacial Physics and Technology, Shanghai Institute of Applied Physics, Chinese Academy of Sciences, Shanghai, 201800, PR China
[c] UNIST Central Research Facilities and School of Materials Science and Engineering, Ulsan National Institute of Science and Technology (UNIST), Ulsan, 44919, Republic of Korea
[d] Materials & Devices Advanced Research Institute, LG Electronics, Seoul, Republic of Korea
[e] Department of Mechanical Engineering, Kumoh National Institute of Technology, Gyeongbuk, 39177, Republic of Korea

ARTICLE INFO

Keywords:
Dry forming of methane
Exsolution
Yttria-stabilized zirconia (YSZ)
Ni nanoparticle

ABSTRACT

Ni nanocatalysts produced through exsolution have shown strong resistance to particle sintering and carbon coking in a beneficial dry reforming of methane (DRM) reaction utilizing greenhouse gases such as CH_4 and CO_2. However, most of the existing oxide supports for exsolution have been limited to perovskite oxide, while studies on fluorite support have been rarely conducted due to the limited solubility despite its excellent redox stability. Here we demonstrate that 3 mol% Ni can be successfully dissolved into the yttria-stabilized zirconia (YSZ) lattice and be further exsolved to the surface in a reducing atmosphere. The YSZ decorated with exsolved Ni nanoparticles shows enhanced catalytic activity for DRM reaction compared to the conventional cermet type of bulk Ni-YSZ. Moreover, the catalytic activity is extremely stable for about 300 h without significant degradation. Overall results suggest that the YSZ-based fluorite structure can be utilized as one of the support oxides for exsolution.

Dry reforming of methane (DRM) has been widely used to utilize two major greenhouse gases such as CO_2 and CH_4 through converting those into syngas (a mixture of hydrogen and carbon monoxide), which is a valuable feedstock for Fischer-Tropsch process and methanol synthesis.[1,2] Although Ni-based catalysts have been considered as a promising alternative to noble metal catalysts for the DRM reaction, deactivation of catalysts in the operating environment remains a major hurdle for the use as a durable catalyst in industrial applications. The main causes of the deactivation are attributed to (1) catalyst sintering in a high operating temperature or (2) carbon deposition on the active site during the reaction.[3–5] Possible strategies for resolving the issues may include adjusting the particle size of catalyst,[6,7] developing support with strong metal-support interaction,[1] and adding promoters.[4,8]

Among many approaches, exsolution which has been extensively studied in the past decade can provide strong metal-support interaction and resistance to particle aggregation to alleviate the deactivation.[9–12] This method allows the in situ growth of metal nanocatalysts on the surface from the cationic form in a crystal lattice of the oxide support in reducing conditions. Since nanoparticles formed via exsolution are socketed on the oxide surface, they have strong interaction with the parent oxide, thereby providing a good thermal stability and carbon coking resistance compared to existing nanoparticle synthesis methods (e.g., wet impregnation or vapor deposition).[13,14] Socketed metal nanoparticles hardly separate from the support oxide due to the base-growth

* Corresponding author.
** Corresponding author.
E-mail address: gtkim@unist.ac.kr (G. Kim).

Production and Hosting by Elsevier on behalf of KeAi

[1] These authors contributed equally to this work.

https://doi.org/10.1016/j.matre.2021.100021
Received 11 August 2020; Received in revised form 12 January 2021; Accepted 11 March 2021
Available online 29 March 2021

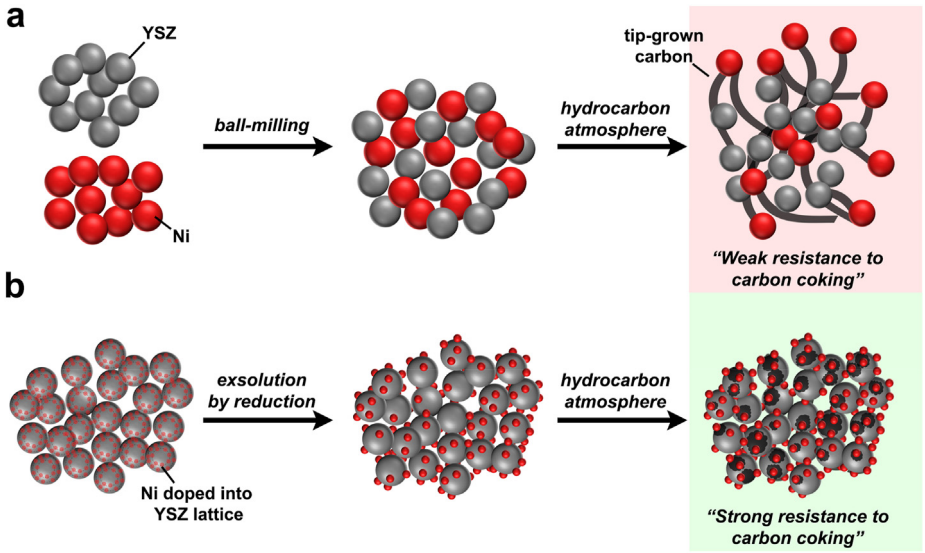

Fig. 1. Schematic comparison of (a) bulk Ni-YSZ blend and (b) dissolved/exsolved Ni-YSZ.

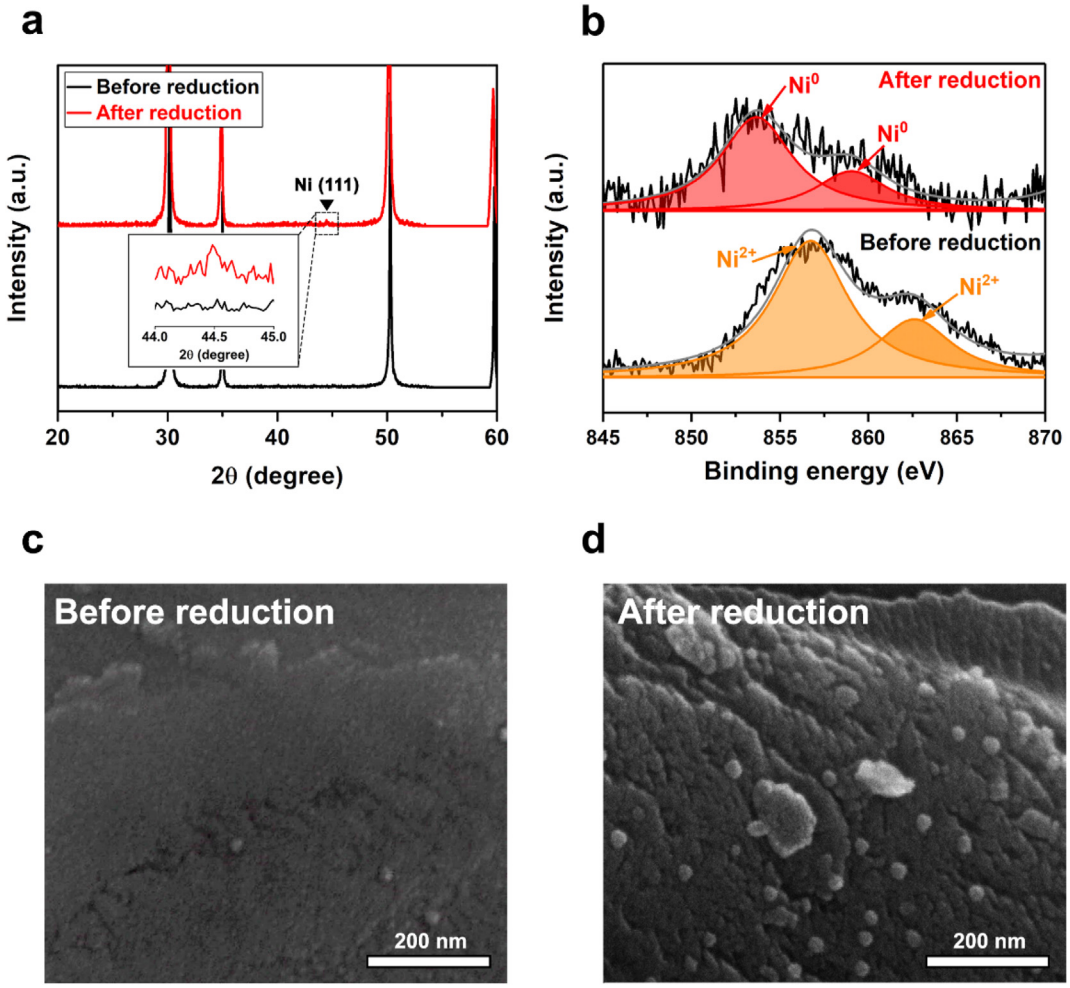

Fig. 2. (a) X-ray diffraction patterns of Ni-doped YSZ before and after reduction. (b) X-ray photoelectron curves of Ni-doped YSZ before and after reduction. SEM images of Ni-doped YSZ (c) before and (d) after reduction.

of carbon at the metal tip and thus agglomeration between particles can be suppressed, securing carbon coking resistance.

Perovskite oxide (ABO_3)[15] and derived materials (e.g., double perovskite ($A_2B_2O_{5+\delta}$),[12,16,17] Ruddlesden Popper (RP, $A_{n+1}B_nO_{3n+1}$)[18,19]) have been widely used as support oxides. Since the structures have excellent redox stability and exsolution feasibility to

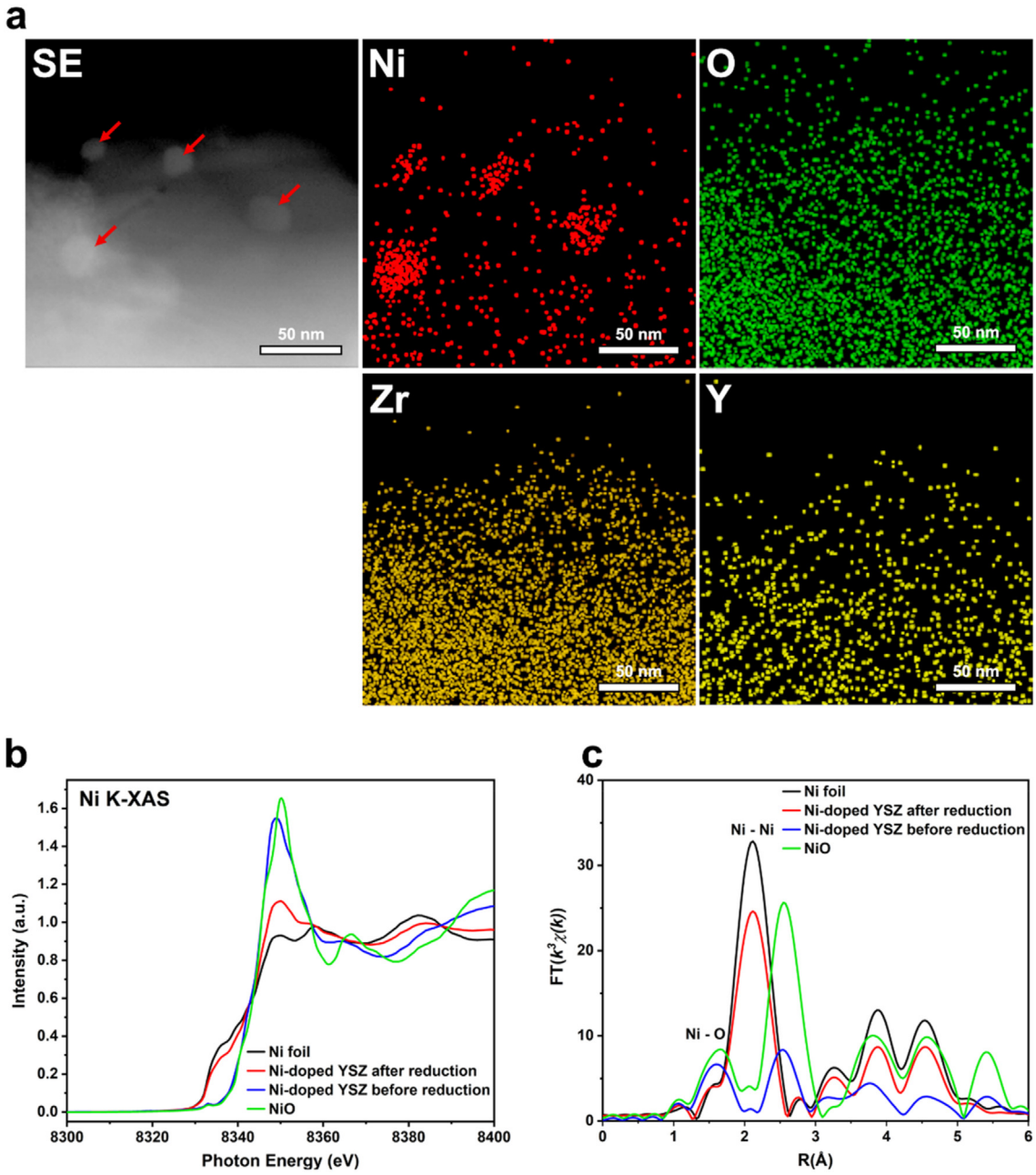

Fig. 3. (a) Transmission electron microscopy of exsolved Ni-YSZ and EDS elemental maps of Ni, O, Zr, and Y (scale bar 50 nm). (b) Ni K-edge XANES and (c) EXAFS spectra of samples.

doping various types of ions into the lattice, they are regarded as suitable exsolution supports. Meanwhile, fluorite-based oxides (e.g., Ce-based fluorite and yttria-stabilized zirconia (YSZ)) have also shown their favorable redox stability. Particularly in the case of YSZ, larger Y^{3+} ions are partially substituted with Zr^{4+} ions to prevent a rapid phase transition varying with the temperature and thus YSZ has very suitable conditions as support for exsolution. However, they have been rarely considered as a support oxide for exsolution to date due to its limited solubility of transition metal (e.g., Ni) into the YSZ lattice.[20,21]

In this work, we attempt for the first time to dissolve Ni into YSZ lattice and to grow homogeneously Ni nanoparticles on the oxide surface in a reducing atmosphere. The overall experimental process and the schematic of carbon coking resistance are illustrated in Fig. 1 to compare with the conventional Ni-YSZ cermets. We demonstrate that about 3 mol % Ni can be dissolved into the YSZ lattice at a temperature of 1600 °C, and when reduced in the H_2 atmosphere, the metallic nanoparticles of Ni can be exsolved on the surface of YSZ while maintaining good redox stability. The YSZ catalyst decorated with exsolved Ni nanoparticles shows excellent catalytic activity for the DRM reaction and does not show any noticeable degradation in the continuous DRM reaction for 300 h at 800 °C. Our results demonstrate that YSZ-based fluorite structures can be employed as support for exsolution and thus could be used as a durable DRM catalyst.

To investigate the structural information of the catalysts, X-ray diffraction was measured before and after reduced Ni-doped YSZ as shown in Fig. 2a. The XRD pattern of Ni-doped YSZ before reduction presents only the YSZ phase of fluorite structure, suggesting that 3 mol% Ni is successfully dissolved in the lattice of YSZ at 1600 °C. After reduction, Ni metal (111) peak was observed at 44.5° which can be evidence of Ni metal exsolution on YSZ lattice. The exsolution of Ni metal is

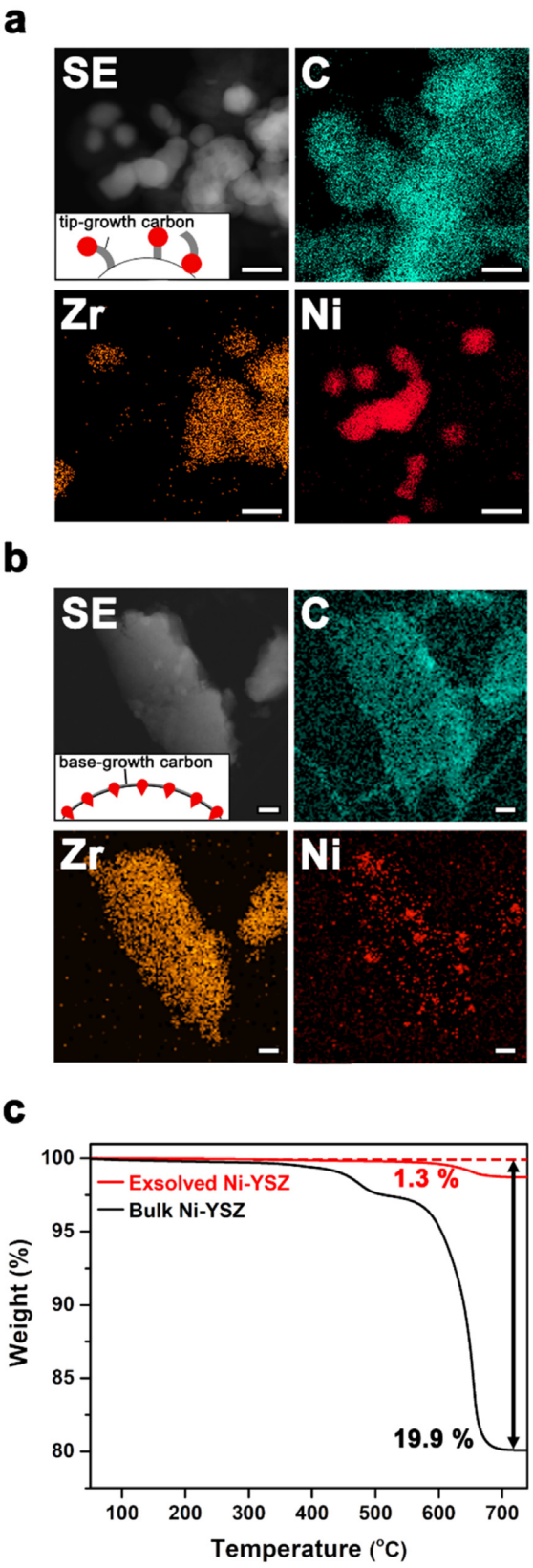

Fig. 4. Transmission electron microscopy and EDS elemental maps of (a) bulk Ni-YSZ and (b) exsolved Ni-YSZ after exposed in CH_4 at 800 °C for 40 h (scale bars are 100 nm), and (c) thermal gravimetric analysis (TGA) results of exsolved/bulk Ni-YSZ after exposed in CH_4 at 800 °C for 40 h.

also confirmed by XPS analysis, as shown in Fig. 1b. The Ni^{2+} peaks of as-prepared Ni-doped YSZ (before reduction) were observed at 856.72 eV and 862.60 eV, indicating Ni exists as an oxide form in the YSZ lattice. After reduction, the peaks corresponding to Ni species were shifted to 853.56 eV and 858.74 eV, respectively, suggesting that the Ni^{2+} cation is reduced to the Ni^0 metal.[22] The exsolution of Ni particles is further evidenced by microstructural changes. Fig. 2c and d are the SEM images before and after the reduction of Ni-doped YSZ. Before the reduction, the surface of the Ni-doped YSZ appeared only smooth, whereas the spherical particles with 20–50 nm diameter were formed on the surface after the reduction, which is in line with the XRD and XPS results.

To analyze the constituent of the exsolved particle, the chemical compositions of the samples were measured by transmission electron microscopy (TEM). The exsolved particles appear to be Ni metal based on energy dispersive spectroscopy (EDS) analysis (Fig. 3a). Moreover, elements other than Ni are not exsolved and appear to retain the oxide phase. The elements of Y, Zr, and O are uniformly distributed as a form of oxide, indicating that the support oxide well maintains the redox stability during the reduction. The exsolved particles are approximately 20–50 nm, which is consistent with the SEM results. A formation of the exsolved nanoparticles is also confirmed by X-ray absorption spectroscopy (XAS) measurements. As shown in Fig. 3b, X-ray absorption near-edge structure (XANES) of Ni K edge from the Ni-doped YSZ after/before the reduction is compared to those of reference Ni foil and NiO. The position of the adsorption edge and the line shapes of XANES can reflect the valence state of Ni. The adsorption edge of the Ni-doped YSZ before reduction lies between that of Ni foil and NiO, and the line shape is much closer to that of NiO than Ni foil, which indicates it is mainly composed of Ni^{2+}. In contrast, after the reduction of Ni-doped YSZ, the line shape is more similar to that of Ni foil than NiO, indicating the existence of most Ni as metal. This is further confirmed by the extended X-ray absorption fine structure (EXAFS) data where Ni–Ni scattering peak in the metal phase located at 2.1 Å and Ni–O scattering peak located at 1.6 Å. The results suggests that Ni mainly exists in the form of Ni^{2+} oxides in the Ni-doped YSZ before reduction, while it does in the form of metal phase in the Ni-doped YSZ after reduction, which is consistent with the results of XANES. Therefore, it can be concluded that a considerable amount of metallic Ni is exsolved from the YSZ bulk lattice and this result agrees well with the TEM and SEM results.

To confirm the carbon tolerance and agglomeration durability, exsolved Ni-YSZ and bulk Ni-YSZ were exposed in CH_4 atmosphere at 800 °C for 40 h and their chemical elements were measured by TEM&EDS mapping, as shown in Fig. 4a and b. When the bulk Ni-YSZ was exposed to CH_4, it was confirmed that Ni particles were highly agglomerated. Furthermore, the Ni particles larger than about 100 nm are separated from the YSZ and aggregated. Since unsupported Ni particles tend to agglomerate easily,[23] Ni particles separated from the YSZ support are prone to particle agglomeration. The larger Ni particles produce a large number of carbon fibers, which seem to occur distinctively, so-called 'tip-growth'.[14] In this mechanism, carbon is first dissolved into Ni lattice, so that carbon fiber could grow at the interface of metal particle-oxide support, consequently resulting in uplifting from its original position. As shown in Fig. 4a, it can be confirmed that grown carbon fibers are formed along with agglomerated Ni particles. On the other hand, the exsolved Ni-YSZ could maintain the initial morphology and particle size of the Ni because the physically anchored Ni particles would prevent the migration of Ni particles and consequently hinder particle agglomeration.[14,17] Moreover, this anchored structure also provides strong carbon coking resistance by the base-growth of carbon rather than the tip-growth.[14] As shown in Fig. 4b, carbon was produced in a widespread shape along with the support oxide, which means that the exsolved Ni particles possess improved carbon coking resistance. To quantitatively evaluate the amount of carbon accumulation, we performed a TGA analysis of the CH_4 exposed exsolved Ni-YSZ and bulk Ni-YSZ samples (Fig. 4c). The weight change during increasing temperature is considered as the weight change of carbon species while they

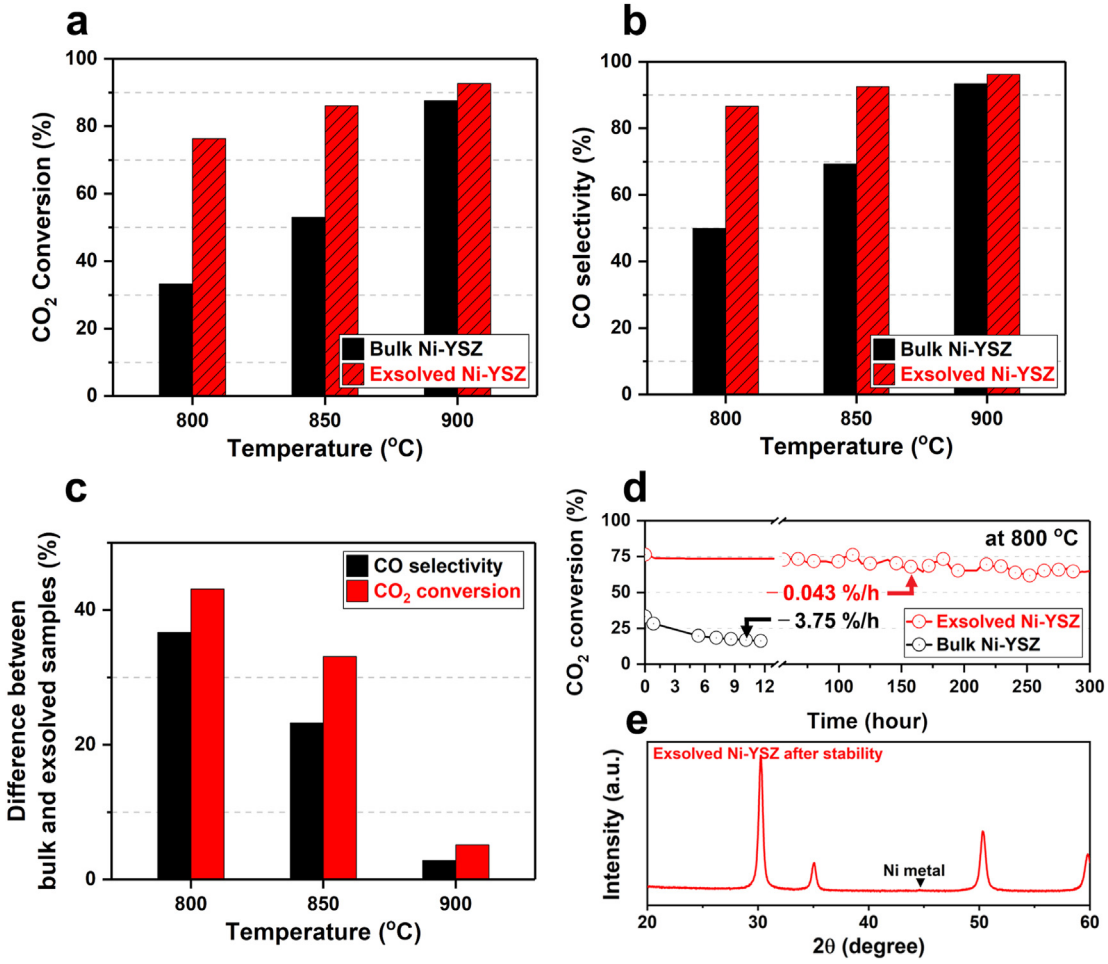

Fig. 5. Catalytic properties of bulk Ni-YSZ and exsolved Ni-YSZ samples. (a) CO_2 conversion, (b) CO selectivity, (c) difference of CO_2 conversion and CO selectivity, and (d) time-dependence of CO_2 conversion of bulk Ni-YSZ and exsolved Ni-YSZ samples. (e) X-ray diffraction patterns of exsolved Ni-YSZ after the stability test.

oxidize. The accumulated carbon amount of exsolved Ni-YSZ is 1.3 wt%, which is much lower than that of bulk Ni-YSZ of 19.9 wt%. This result is well consistent with TEM images (Fig. 4a and b). Therefore, the base-growth of carbon is more effective than tip-growth carbon in terms of preventing Ni particle agglomeration and carbon accumulation.

The catalytic activities of the samples for DRM are evaluated using the quartz tube reactor and gas chromatography (GC). As shown in Fig. 5a, the CO_2 conversion value of the exsolved Ni-YSZ is higher at all measured temperatures than that of bulk Ni-YSZ. The results may be attributed to the extended surface area of exsolved Ni-YSZ obtained by uniformly distributed nano-sized Ni particles on the YSZ surface. The CO_2 conversion values at a high temperature of 900 °C of exsolved Ni-YSZ are 92.7%, slightly higher than that of bulk Ni-YSZ of 87.6%. This difference is narrowed sharply compared to the results obtained at lower temperatures (800 °C and 850 °C). In particular, at 800 °C, the CO_2 conversion value for exsolved Ni-YSZ and Bulk Ni-YSZ are about 76.4% and 33.3%, respectively. It is confirmed that the exsolved Ni-YSZ sample exhibits a 2-fold higher catalytic activity than the bulk Ni-YSZ at 800 °C. The CO_2 conversion values at 900 °C are similar for the two samples, and the difference gradually enlarges as temperature decreases. This seems to be due to the difference in the size of the Ni metal particles between the exsolved Ni-YSZ sample and the bulk Ni-YSZ sample, and the difference in the degree of support by oxides.[24] In the DRM reaction, the well dispersed particles supported on the support can contribute to CO_2 activation at low temperatures.[25] As confirmed in the TEM image (Figs. 3a and 4b), in the case of the exsolved Ni-YSZ sample, about 20 nm of Ni particles are well dispersed and supported on the support, whereas, in the bulk Ni-YSZ, Ni particles are relatively agglomerated with a size of about 80 nm. In general, it is known that the smaller the size of metal nanoparticles and the larger the dispersion, the higher the activity and the enhanced stability for carbon.[24,26] Therefore, the exsolved Ni-YSZ sample appears to have high activity at low temperature due to metal size in addition to the morphological characteristics of exsolution. Furthermore, as the temperature decreases, the Boudouard reaction becomes more favorable, which can be a factor in the formation of carbon. The Boudouard reaction is an exothermic reaction that rarely occurs above the temperature of 900 °C, but at a relatively lower temperature (800 °C), deactivation of catalysts caused by carbon may occur. This is shown to be insignificant in the exsolved Ni-YSZ, while a significant amount of carbon starts to grow in the bulk Ni-YSZ. The stability of dry reforming of methane was also evaluated (Fig. 5d). The exsolved Ni-YSZ shows excellent stability of 0.043%/h degradation rate over 300 h while the bulk Ni-YSZ exhibits a degradation rate of 3.75%/h only in 10 h at 800 °C. In exsolution, since the metal lattice grows from the oxide lattice, interdiffusion between the metal and the oxide lattice can occur at the interface, which in turn significantly increases the adhesion between the two materials.[14] As a result, this structure seems to contribute to considerably improving the anchorage of exsolved particles. On the other hand, in the case of conventional nanoparticles through deposition or mixing, the interaction between the particles and oxide phases is not strong, which can explain the difference in stability. The sustained Ni nano-size particles by the unique anchored structure are also confirmed by the TEM images and TGA results. The CO_2 conversion and stability duration of the recently studied DRM catalysts are compared with that of

Table 1
CO_2 conversion comparison with selected DRM catalysts.

Catalyst	Ni content to cations (mol%)	Time (hours)	CO_2 conversion (%)	Gas composition (CH_4:CO_2)	Ref.
$NiMo_2C@La_2O_3$	33.3	50	70	1:1	[25]
$Pt/Ce–ZrO_2$	–	20	35	2:1	[27]
$CaZr_{0.8}Ni_{0.2}O_{3-\delta}$	10	500	96	1:1	[28]
$Ni–SiO_2$	100	170	52.8	1:1	[6]
$LaNiO_3$	50	50	80	1:1	[29]
PBMNi-12-Fe	7.5	100	15	1:1	[9]
Exsolved Ni-YSZ	3	300	76	1:1	This work

exsolved Ni-YSZ as shown in Table 1. Considering that the Ni content of the exsolved Ni-YSZ sample is only about 3 mol% of the total cations, the CO_2 conversion and stability of the sample are considered to be highly excellent.

In conclusion, despite the difficulties from the limited solubility of the YSZ lattice, we have successfully demonstrated the exsolution phenomenon of Ni from the YSZ substrate and characterized its catalytic activity for dry reforming of methane. The exsolved Ni nanoparticles not only improve the catalytical activity by the extension of the catalytically active site but also show very strong tolerance for agglomeration by unique anchors structure. This improvement can be reflected on the catalytic activity for DRM. The catalytic activity of exsolved Ni-YSZ for DRM is improved about 2-fold higher compared to that of bulk Ni-YSZ at 800 °C with highly enhanced stability of 0.043%/h degradation rate.

Declaration of competing interest

There are no conflicts to declare.

Acknowledgments

This work was supported by the Korea Institute of Energy Technology Evaluation and Planning (KETEP) and the Ministry of Trade, Industry & Energy (MOTIE) of the Republic of Korea (No. 20173020032120). This work also was supported by the Basic Science Research Program through the National Research Foundation of Korea (NRF) funded by the Ministry of Education (NRF-2019R1C1C1005801). Partial support from "CO_2 utilization battery for hydrogen production based on fault-tolerance deep learning" (1.200097.01) is also acknowledged.

Appendix A. Supplementary data

Supplementary data to this article can be found online at https://doi.org/10.1016/j.matre.2021.100021.

References

1. Song Y, Ozdemir E, Ramesh S, et al. Dry reforming of methane by stable Ni-Mo nanocatalysts on single-crystalline MgO. *Science*. 2020;367(6479):777–781. https://doi.org/10.1126/science.aav2412.
2. Pakhare D, Spivey J. A review of dry (CO_2) reforming of methane over noble metal catalysts. *Chem Soc Rev*. 2014;43(22):7813–7837. https://doi.org/10.1039/C3CS60395D.
3. Liang TY, Lin CY, Chou FC, Wang M, Tsai DH. Gas-phase synthesis of Ni-CeOx hybrid nanoparticles and their synergistic catalysis for simultaneous reforming of methane and carbon dioxide to syngas. *J Phys Chem C*. 2018;122(22):11789–11796. https://doi.org/10.1021/acs.jpcc.8b00665.
4. Das S, Ashok J, Bian Z, et al. Silica–Ceria sandwiched Ni core–shell catalyst for low temperature dry reforming of biogas: coke resistance and mechanistic insights. *Appl Catal B Environ*. 2018;230(November 2017):220–236. https://doi.org/10.1016/j.apcatb.2018.02.041.
5. Liu Z, Grinter DC, Lustemberg PG, et al. Dry reforming of methane on a highly-active Ni-CeO2Catalyst: effects of metal-support interactions on C−H bond breaking. *Angew Chem Int Ed*. 2016;55(26):7455–7459. https://doi.org/10.1002/anie.201602489.
6. Han JW, Kim C, Park JS, Lee H. Highly coke-resistant Ni nanoparticle catalysts with minimal sintering in dry reforming of methane. *ChemSusChem*. 2014;7(2):451–456. https://doi.org/10.1002/cssc.201301134.
7. Chai Y, Fu Y, Feng H, et al. A nickel-based perovskite catalyst with a bimodal size distribution of nickel particles for dry reforming of methane. *ChemCatChem*. 2018;10(9):2078–2086. https://doi.org/10.1002/cctc.201701483.
8. Theofanidis SA, Galvita VV, Poelman H, Marin GB. Enhanced carbon-resistant dry reforming Fe-Ni catalyst: role of Fe. *ACS Catal*. 2015;5(5):3028–3039. https://doi.org/10.1021/acscatal.5b00357.
9. Joo S, Kwon O, Kim S, Jeong HY, Kim G. Ni-Fe bimetallic nanocatalysts produced by topotactic exsolution in Fe deposited $PrBaMn_{1.7}Ni_{0.3}O_{5+\delta}$ for dry reforming of methane. *J Electrochem Soc*. 2020;167, 064518. https://doi.org/10.1149/1945-7111/ab8390.
10. Abdulrasheed A, Jalil AA, Gambo Y, Ibrahim M, Hambali HU, Shahul Hamid MY. A review on catalyst development for dry reforming of methane to syngas: Recent advances. *Renew Sustain Energy Rev*. 2019;108(April):175–193. https://doi.org/10.1016/j.rser.2019.03.054.
11. Kwon BW, Oh JH, Kim GS, et al. The novel perovskite-type Ni-doped Sr0.92Y0.08TiO3 as a reforming biogas ($CH_4 + CO_2$) for H_2 production. *Appl Energy*. 2018;227(July 2017):213–219. https://doi.org/10.1016/j.apenergy.2017.07.105.
12. Joo S, Kwon O, Kim K, et al. Cation-swapped homogeneous nanoparticles in perovskite oxides for high power density. *Nat Commun*. 2019;10(1):697. https://doi.org/10.1038/s41467-019-08624-0.
13. Lai K-Y, Manthiram A. Self-regenerating Co−Fe nanoparticles on perovskite oxides as a hydrocarbon fuel oxidation catalyst in solid oxide fuel cells. *Chem Mater*. 2018;30(8):2515–2525. https://doi.org/10.1021/acs.chemmater.7b04569.
14. Neagu D, Oh TS, Miller DN, et al. Nano-socketed nickel particles with enhanced coking resistance grown in situ by redox exsolution. *Nat Commun*. 2015;6:8120. https://doi.org/10.1038/ncomms9120.
15. Neagu D, Tsekouras G, Miller DN, Menard H, Irvine JTS. In situ growth of nanoparticles through control of non-stoichiometry. *Nat Chem*. 2013;5(11):916–923. https://doi.org/10.1038/nchem.1773.
16. Kwon O, Sengodan S, Kim K, et al. Exsolution trends and co-segregation aspects of self-grown catalyst nanoparticles in perovskites. *Nat Commun*. 2017;8(May):15967. https://doi.org/10.1038/ncomms15967.
17. Kwon O, Kim K, Joo S, et al. Self-assembled alloy nanoparticles in layered double perovskite as a fuel oxidation catalyst for solid oxide fuel cells. *J Mater Chem*. 2018;6(33):15947–15953. https://doi.org/10.1039/C8TA05105D.
18. Du Z, Zhao H, Yi S, et al. High-performance anode material $Sr_2FeMo_{0.65}Ni_{0.35}O_{6-\delta}$ with in situ exsolved nanoparticle catalyst. *ACS Nano*. 2016;10:8660–8669. https://doi.org/10.1021/acsnano.6b03979.
19. Kim KJ, Rath MK, Kwak HH, et al. A highly active and redox-stable $SrGdNi_{0.2}Mn_{0.8}O_{4\pm\delta}$ anode with in situ exsolution of nanocatalysts. *ACS Catal*. 2019;9(2):1172–1182. https://doi.org/10.1021/acscatal.8b03669.
20. Skarmoutsos D, Nikolopoulos P, Tsoga A. Titania doped YSZ for SOFC anode Ni-cermet. *Ionics (Kiel)*. 1999;5(5-6):455–459. https://doi.org/10.1007/BF02376013.
21. Satardekar P, Montinaro D, Sglavo VM. Fe-doped YSZ electrolyte for the fabrication of metal supported-SOFC by co-sintering. *Ceram Int*. 2015;41(8):9806–9812. https://doi.org/10.1016/j.ceramint.2015.04.053.
22. Song Y, Wang W, Ge L, et al. Rational design of a water-storable hierarchical architecture decorated with amorphous barium oxide and nickel nanoparticles as a solid oxide fuel cell anode with excellent sulfur tolerance. *Adv Sci*. 2017;1700337:1700337. https://doi.org/10.1002/advs.201700337.
23. Toebes Ml, Bitter JH, Dillen AJ Van, Jong KP de. Impact of the structure and reactivity of nickel particles on the catalytic growth of carbon nanofibers. *Catal Today*. 2002;76:33–42.
24. ying Jing J, hua Wei Z, Zhang Y bin, cun Bai H, ying Li W. Carbon dioxide reforming of methane over MgO-promoted Ni/SiO2 catalysts with tunable Ni particle size. *Catal Today*. 2020;356(January):589–596. https://doi.org/10.1016/j.cattod.2020.01.006.
25. Zhang S, Shi C, Chen B, et al. Catalytic role of β-Mo2C in DRM catalysts that contain Ni and Mo. *Catal Today*. 2015;258:676–683. https://doi.org/10.1016/j.cattod.2015.01.014.
26. Bian Z, Das S, Wai MH, Hongmanorom P, Kawi S. A review on bimetallic nickel-based catalysts for CO_2 reforming of methane. *ChemPhysChem*. 2017;18(22):3117–3134. https://doi.org/10.1002/cphc.201700529.
27. Stagg-Williams SM, Noronha FB, Fendley G, Resasco DE. CO_2 reforming of CH_4 over Pt/ZrO_2 catalysts promoted with La and Ce oxides. *J Catal*. 2000;194(2):240–249. https://doi.org/10.1006/jcat.2000.2939.
28. Dama S, Ghodke SR, Bobade R, Gurav HR, Chilukuri S. Active and durable alkaline earth metal substituted perovskite catalysts for dry reforming of methane. *Appl Catal B Environ*. 2018;224(October 2017):146–158. https://doi.org/10.1016/j.apcatb.2017.10.048.
29. Nair MM, Kaliaguine S, Kleitz F. Nanocast $LaNiO_3$ perovskites as precursors for the preparation of coke-resistant dry reforming catalysts. *ACS Catal*. 2014;4(11):3837–3846. https://doi.org/10.1021/cs500918c.

Sangwook Joo is going to receive his PhD degree from the Department of Energy Engineering, Ulsan National Institute of Science and Technology (UNIST) in 2021. His current research is mainly focused on perovskite oxide based nanocatalysts for electrochemical and thermochemical devices.

Chaehyun Lim received his PhD degree from the Department of Energy Engineering, Ulsan National Institute of Science and Technology (UNIST) in 2021. He investigates electrochemical devices such as solid oxide fuel cell and metal air batteries.

Sihyuk Choi is an Assistant Professor in Department of Mechanical Engineering at Kumoh National Institute of Technology, Republic of Korea. He received his PhD (2015) in Ulsan National Institute of Science and Technology, Republic of Korea. He completed his postdoctoral research from 2015 to 2018 at Prof. Sossina Haile group at Caltech and Northwestern University, USA. His current research interests are primarily focused on advanced materials for electrochemical energy conversion and storage devices, including ceramic based fuel cells and electrolysis cells.

Guntae Kim is currently a professor of School of Materials Science and Engineering, Department of Energy Engineering, Ulsan National Institute of Science and Technology (UNIST). His research interests are energy conversion and strage devices such as solid oxide fuel cells, solid oxide electrolyzer, metal-air batteries, polymer electrolyte membrane fuel cells, oxygen membrane reactor, direct carbon fuel cells, and proton conducting oxides based on the studies of perovskite-type material.